Evolution of craniofacial shape in relation to sexual dimorphism in *Theropithecus* and *Papio*

Ángeles Ossorio[1], Ambra Figueroa-Torrejón[2], Rodrigo Buston[1], Matteo Caldon[3], Jacinto Mathe[4,5], Giuliano Doria[6], Spartaco Gippoliti[7,8], Antonella Volta[9], María Joana Ferreira da Silva[10,11,12], René Bobe[4,5,13], Susana Carvalho[4,5,10,13], Cristian Capelli[3] and Felipe I. Martínez[14]*

[1]Facultad de Ciencias Biológicas, Pontificia Universidad Católica de Chile, Santiago, Chile, [2]Physical Anthropology Unit, Department of Biodiversity, Ecology, and Evolution, Faculty of Biological Sciences, Universidad Complutense de Madrid, Madrid, Spain, [3]Department of Chemistry, Life Sciences and Environmental Sustainability, University of Parma, Parma, Italy, [4]Department of Science, Gorongosa National Park, Sofala, Mozambique, [5]Institute of Human Sciences, School of Anthropology and Museum Ethnography, University of Oxford, Oxford, United Kingdom, [6]Museo Civico di Storia Naturale "Giacomo Doria", Genoa, Italy, [7]IUCN/SSC Primate Specialist Group, Rome, Italy, [8]Società Italiana per la Storia della Fauna "G. Altobello", Rome, Italy, [9]Department of Veterinary Science, University of Parma, Parma, Italy, [10]CIBIO, Centro de Investigação em Biodiversidade e Recursos Genéticos, InBIO Laboratório Associado Campus de Vairão, Universidade do Porto, Vairão, Portugal, [11]BIOPOLIS Program in Genomics, Biodiversity and Land Planning, CIBIO, Vairão, Portugal, [12]Organisms and Environment Division, School of Biosciences, Cardiff University, Cardiff, United Kingdom, [13]Interdisciplinary Center for Archaeology and Evolution of Human Behaviour (ICArEHB), University of Algarve, Faro, Portugal, [14]Escuela de Antropología, Facultad de Ciencias Sociales, Pontificia Universidad Católica de Chile, Santiago, Chile

Introduction: Sexual dimorphism in cranial morphology is a significant aspect of primate evolution, providing insights into evolutionary pressures and mating systems in different species. This study focuses on cranial sexual dimorphism in *Papio* and *Theropithecus*, two closely related genera within the tribe Papionini.

Methods: Using geometric morphometric techniques, we analyzed 570 cranial specimens from both genera, with data sourced from various studies and repositories. Thirty craniofacial landmarks were defined and analyzed through Geometric Morphometrics tools to evaluate shape variation.

Results: Our findings reveal distinct morphological clusters for each genus and sex, with *Papio* and *Theropithecus* exhibiting significant sexual dimorphism. The results distinguish genera and sex-based groups, indicating differential impacts of size on shape across groups. The findings suggest that while sexual dimorphism is stable in magnitude within each genus, the specific morphological manifestations differ.

Discussion: This research advances our understanding of the evolutionary mechanisms driving sexual dimorphism and emphasizes the need for further studies to explore the genetic and environmental factors influencing these differences. The innovative approach and comprehensive dataset provide a robust framework for future investigations into primate cranial morphology and its evolutionary implications.

Introduction

Sexual dimorphism is a significant aspect influencing morphological variability and evolution in primates. All African papionins, which include the genera *Cercocebus* and *Lophocebus* (mangabeys), *Mandrillus* (mandrills and drills), *Papio* (baboons), *Rungwecebus* (kipunji) and *Theropithecus* (geladas) (Strasser and Delson, 1987; Zinner et al., 2013), are characterized by being sexually dimorphic, resulting in significantly different morphologies between males and females (Delson et al., 2000; Smith and Jungers, 1997). In the case of *Mandrillus*, females account for 30%-40% of male size, while in the others, they correspond to 50%-70% of male size (Swedell, 2011). Large-bodied papionins, *Mandrillus, Papio* and *Theropithecus*, share a series of morphological characteristics such as a high degree of terrestriality, elongated faces with prominent snout, and being some of the most visually striking with varied colorations and showy manes, hypothesized to have evolved through sexual selection (Setchell and Dixson, 2001; Setchell, 2005; Swedell, 2011). From this, they are considered a good model for evaluating the dynamics of sexual selection and its mechanisms, because closely related species exhibit pronounced variations in sexually selected traits (Petersdorf et al., 2019).

At the phylogenetic level, molecular data indicate that large-bodied papionins do not form a monophyletic clade, despite sharing many morphological characteristics. Instead, mandrills are phylogenetically grouped with *Cercocebus*, while baboons cluster with geladas, arboreal mangabeys (*Lophocebus*) and kipunji (Liedigk et al., 2014; Pugh and Gilbert, 2018; Craig et al., 2024). It has been suggested that, in addition to this closeness, episodes of intergeneric introgression have occurred between baboons and geladas during their evolutionary history (Walker et al., 2019; Caldon et al., 2024), with interbreeding reported in extant wild and captive populations (Dunbar and Dunbar, 1974; Harris and Disotell, 1998; Zinner et al., 2011).

Baboons (*Papio* sp.) have successfully adapted to diverse habitats, and currently inhabit the coastal areas of the Red Sea in the Arabian Peninsula and sub-Saharan Africa (Fleagle, 2013). Six species of *Papio* are presently recognized under the phylogenetic species concept: *P. anubis* (olive), *P. cynocephalus* (yellow), *P. hamadryas* (hamadryas), *P. kindae* (kinda), *P. papio* (Guinea), and *P. ursinus* (chacma) (Zinner et al., 2009, 2013). *Papio* species exhibit a wide range of behavioral patterns and are phenotypically different (Elton and Dunn, 2020). They show differences in body size, cranial morphology, color and texture of adult coat, and sexually selected characteristics such as sexually dimorphic canines (Fischer et al., 2019; Martinez et al., 2019).

The genus *Theropithecus* has only one extant species, *T. gelada*, with three apparently distinct evolutionary units inhabiting the highlands of Ethiopia (Gippoliti, 2010; Shotake et al., 2016; Zinner et al., 2018; Snyder-Mackler et al., 2014; Trede et al., 2020; Caldon et al., 2024). They live in complex, multi-level societies with units composed of a reproductive leader male, several adult females and their young, which then group with other units forming bands, which in turn group into communities or herds (Snyder-Mackler et al., 2012). This species exhibits a high degree of sexual dimorphism in body size (males weigh on average 16.5-20.5 kg, and females 8.3-13.8 kg) and appearance, with males having long, shaggy hair, pronounced facial whiskers, and large canines, while females have shorter coat and more uniform color (Bergman and Beehner 2013; Fleagle, 2013).

Geladas, hamadryas and Guinea baboons maintain a complex multilevel social organization system, where the primary level of organization of their society is the one-male unit, which corresponds to the reproductive unit composed of a sexually active male leader, a variable number of adult females (1–12 in geladas; 1–6 in Guinea), their offspring and, in some cases, 1 or 2 follower males (Fleagle, 2013; Kummer, 1968). When several units join together, they form clans, which in turn to constitute bands, and finally, these gather into communities or troops around resources such as sleeping sites (Fleagle, 2013; Schreier and Swedell, 2009). However, they differ in that both baboon species exhibit male philopatry with limited female dispersal from groups, whereas geladas display female philopatry with male dispersal from the natal unit (Jolly, 2020; Fischer et al., 2017; Snyder-Mackler et al., 2014). They are characterized by polygyny, with intense competition for female mates, as the group's leader male aggressively excludes others and monopolizes females, protecting his access to mating and offspring (Chowdhury et al., 2015; Kummer, 1968; Pines et al., 2011).

In contrast, chacma, olive, kinda and yellow baboons, known as savannah baboons and dubbed "COKY" baboons (Jolly, 2020), live in multi-male, multi-female groups (parsimoniously hypothesized as ancestral state of the genus) with female philopatry and male dispersal, where females remain in the group, constituting its stable core, and males leave it to join a new one (Fischer et al., 2019). Their mating system is polygynandrous, meaning that both females and males have multiple mating partners (Fischer et al., 2017, 2019), nevertheless, high-ranking males tend to have greater mating and reproductive success, with this bias manifesting more in chacma baboons (Bulger, 1993; Alberts et al., 2003, 2006). However, there is great variation in their degree of sexual dimorphism, reflecting differences in the intensity of male competition and female mate choice (Petersdorf et al., 2019).

The genus *Papio* shows a pronounced variation in the degree and expression of other sexual traits (Dixson, 2012). An example of this is body mass, which can range between 17–30 kg in males and 9–16 kg in females, resulting in a ratio that varies between 1.56 and 2.00 (Delson et al., 2000; Dunbar, 1990; Fischer et al., 2017; Swedell, 2011). The kinda baboon is the smallest and most gracile baboon species, exhibiting the least sexual dimorphism in body size (Singleton et al., 2017; Petersdorf et al., 2019), while the chacma baboon is the largest baboon species with the greatest size difference between sexes (Jolly et al., 2011). Additionally, *Papio* species in multi-level/one-male unit (polygynous males) and multi-male-multi-female (polygynandrous) systems differ in their growth rates. Polygynous males in the former group (*P. papio* and *P. hamadryas*) tend to accelerate and shorten their growth (thus growing less). While polygynandrous males in the latter group of species (*P. anubis, P. ursinus* and *P. cynocephalus*) are more likely to

reach a larger body size (Leigh et al., 2005). An exception to this is *P. kindae*, which despite belonging to the second group of baboons, their growth patterns differ due to differences in their allometry patterns and size related to shape dimorphism (Singleton et al., 2017). It can also be observed that adult males of savannah baboons either lack or have moderately fur capes, whereas hamadryas and Guinea baboons have prominent capes with multiple light and dark rings (Jolly, 2020; Petersdorf et al., 2019). Also, differences in relative testis size have been described, with polygynous species having smaller adult testis size compared to baboons living in multi-male, multi-female groups, with larger testis, probably being selected for in polygynandrous primates (Dixson, 2017).

In most primates and mammals, the observed male-biased sexual size dimorphism, such as in *Papio* and *Theropithecus*, mirrors the strength of sexual selection acting upon males. In the past, morphometrics studies of the *Papio* skull have shown that the variation in baboons is influenced by various factors that reflect adaptations to local selection (Leigh and Cheverud, 1991). However, sexual selection and male competition are the default hypotheses to explain the pronounced dimorphism of the craniofacial skeleton, in particular canines (Leigh, 2006). Sexual selection could be partly responsible for the evolution of other secondary traits in male baboons or to contribute to female size, thus driving specific morphological divergence within and between genera (Gilbert et al., 2009; Leigh, 2006). Moreover, all these male-biased traits are likely to be informative at the phylogenetic level if they correlate to shared mating systems (Gilbert and Rossie, 2007).

Male and female baboons follow a common ontogenetic trajectory during their developmental stages, and in some cases juvenile cranial forms are indistinguishable between sexes (Collard and O'Higgins, 2001; Simons et al., 2018). Thus, craniofacial sexual dimorphism is related to size in African cercopithecines (including *Papio* and *Theropithecus*), and in baboons allometric scaling plays an important role (Frost et al., 2003; Leigh and Cheverud, 1991; Leigh, 2006; Singleton, 2002). Allometry plays a significant role in structuring adult morphological diversity, with variables such as the rate and/or duration of cranial growth being particularly important as they substantially contribute to skull shape variation in baboons (Frost et al., 2003; Frost, 2013). This is because males grow at a faster rate and for a longer period than females to reach their final adult size, while females slow their growth much earlier (Leigh and Bernstein, 2006). In relation to canine's sexual dimorphism, it has been found that the male teeth erupts at a later age, at a faster rate and for a longer duration than in females, while in females, it erupts with extraordinary speed (Leigh et al., 2005).

Furthermore, there are species-level differences in the patterns of craniodental sexual dimorphism in *Papio*, as in the case of *P. kindae* (Singleton et al., 2017). Kinda baboons deviate from a common ontogenetic pathway, showing less pronounced size and shape dimorphism than other baboon species. It has even been observed that *P. kindae* adult cranial size and shape are like those of subadults in other baboon species (Petersdorf et al., 2019). Therefore, it has been proposed that less intense sexual selection may contribute to limit dimorphism and size increase in *P. kindae* (Leigh, 2006). However, the pattern of canine dimorphism in *P.

kindae* is common to the mean of other *Papio* species (Singleton et al., 2017). On the one hand, *P. ursinus* exhibits higher canine dimorphism, which reflects the larger size of males (Plavcan, 1998). On the other hand, *P. anubis* presents lower canine dimorphism, which would be linked to increased canine height in females and low dimorphism in cranial shape (Singleton et al., 2017).

Within this context, this study aims to quantitatively evaluate and compare cranial sexual dimorphism between the genera *Papio* and *Theropithecus* by means of geometric morphometrics tools. We aim to describe the size and shape patterns of craniofacial dimorphism, and whether they manifest in the same way or not in these genera. Among the large-bodied papionins, these two genera are the most closely related phylogenetically, enabling new comparative assessments of cranial morphology and the evolution of sexual dimorphism in highly dimorphic and related species.

Materials and methods

Sampling and data acquisition

The study comprises 570 cranial specimens analyzed by means of geometric morphometrics tools using 30 homologous three-dimensional (3D) landmarks. Table 1 shows the composition of the sample, with 519 specimens belonging to the six species of the genus *Papio* and 51 specimens belonging to the genus *Theropithecus*. Among these, the genus *Papio* includes 384 males and 135 females, while the genus *Theropithecus* comprises 29 males and 22 females (Table 1). The sample combines four different sources of data representing the baboon craniofacial skeleton: (a) Dunn et al. (2013) providing 546 individuals with 3D craniofacial landmark coordinates manually recorded from museum specimens using a Microscribe (Dunn et al., 2013; Elton and Cardini, 2008); (b) Martínez et al. (2019) providing 3D surface models from 8 *Papio*

TABLE 1 Composition of the sample.

Number of specimens by sex and species				
Genus	Species	Male	Female	Total
Theropithecus				
	gelada	29	22	51
Papio				
	anubis	116	46	162
	cynocephalus	46	27	73
	hamadryas	35	8	43
	kindae	10	8	18
	papio	13	1	14
	ursinus	67	16	83
	sp	97	29	126
	Total	413	157	570

individuals from Gorongosa National Park, Mozambique (Bobe et al., 2020; Ferreira da Silva et al., 2025; Caldon et al., 2025), these surface models were generated using a Next Engine Desktop 3D Scanner from NextEngine, Inc., and digitized using Amira 5.5 software (Mercury Inc. USA); (c) Morphosource (http://morphosource.org/), a free-access platform (Copes et al., 2016) from where 10 surface models were downloaded and digitized using the Landmark v3.2 software; and (d) new scanning data from 6 individuals from the Museo Storia Naturale di Genova (MSNG), CT-scanned in a Siemens Somatom Sensation Open, multilayer helicoidal Scan (20 layers) and digitized using the Landmark v3.2 program (see Supplementary Table 1 for details).

The set of thirty (3D) landmarks was selected and filtered from the configuration of landmarks used in Dunn et al. (2013) and Martínez et al. (2019). The Table 2 presents the detailed anatomical description of the 30 landmarks used in this study. The landmarks were defined following a protocol that involves eliminating specimens with a low number of recorded points and excluding landmarks absent in a significant portion of the group. This approach allowed for a balanced and representative data set that could be reliably compared across different individuals and species (Figure 1).

Morphometric analysis

Geometric morphometric methods were used to study the variability in cranial shape and size. The landmark-data underwent Generalized Procrustes analysis (GPA) superimposition, minimizing the sum of square Euclidean distances between corresponding landmarks. The scaling method was performed using unit centroid size (Bookstein, 1991; Slice, 2001). Principal Component Analysis (PCA) was used to summarize the variance and visualize the distribution of the entire sample, and for males and females independently. The PCA reduces the dimensionality of the morphometric data to a set of uncorrelated components (PCs) and allows the exploration of distribution trends without prior assumption about classification. Pooled within-groups (species) regression analyses were conducted for males and females to assess the impact of (log) centroid size on cranial shape (Drake and Klingenberg, 2008), and the magnitude of dimorphism was measured using boxplots of centroid size. With the aim to further explore the interaction between size and shape accounting for differences between genera, we followed another two methodological procedures. First, the residuals from the regressions were subjected to a new GPA and PCA. This procedure allows us to explore the differences between *Papio* and *Theropithecus* using shape components that are size-independent. Finally, we performed natural log-centroid size regressions for separate species (including males and females together) to compute shape scores for each of them. The resulting shape scores represent allometric vectors related to sex for each species that can be then compared by assessing the angular relation between them (Singleton et al., 2017; Klingenberg and Marugán-Lobón, 2013). If the observed angle between two vectors is smaller than expected, the two vectors share some degree of similarity between them (Klingenberg and Marugán-Lobón, 2013).

TABLE 2 Anatomical definitions of the thirty, three-dimensional landmarks used in this study.

Anatomical description of the Landmarks used	
Landmark	Description
1	Prosthion: antero-inferior point on projection of pre-maxilla between central incisors.
2	Prosthion2: antero-inferior-most point on pre-maxila, equivalent to prosthion but between central and lateral incisors
3	Anterior-most point of canine alveolus.
4	Mesial p3: Most mesial point on P3 alveolus, projected onto alveolar margin
5	Contact Points between adjacent pre-molars/molars, projected labially onto alveolar margin.
6	Contact Points between adjacent pre-molars/molars, projected labially onto alveolar margin.
7	Contact Points between adjacent pre-molars/molars, projected labially onto alveolar margin.
8	Contact Points between adjacent pre-molars/molars, projected labially onto alveolar margin.
9	Posterior midpoint onto alveolar margin.
10	Contact Points between adjacent pre-molars/molars, projected lingually onto alveolar margin
11	Contact Points between adjacent pre-molars/molars, projected lingually onto alveolar margin.
12	Contact Points between adjacent pre-molars/molars, projected lingually onto alveolar margin.
13	Contact Points between adjacent pre-molars/molars, projected lingually onto alveolar margin.
14	Anterior-most point of the incisive foramen.
15	Middle-line point of the incisive foramen projected onto its margin.
16	Posterior-most point of incisive foramen
17	Greater palatine foramen.
18	Point of maximum curvature on the posterior edge of the palatine.
19	Tip of posterior nasal spine.
20	Anterior tip of the external auditory meatus.
21	Posterior tip of the external auditory meatus.
22	Inion: most posterior point of the cranium.
23	Asterion: Most lateral meeting point of mastoid part of temporal bone and supraoccipital
24	Nasospinale: inferior-most midline point of piriform aperture.
25	Point corresponding to largest width of piriform aperture.
26	Nasion: midline point on fronto-nasal suture.
27	Glabella: Most forward projecting midline point of frontals at the level of the supraorbital ridges.
28	Zygo-max superior:antero-superior point of zygomaticomaxillary suture taken at orbit.

(Continued)

TABLE 2 Continued

Anatomical description of the Landmarks used	
Landmark	Description
29	Center of nasolacrimal foramen (fossa for lacrimal duct)
30	Lambda: Junction of sagital and lamboid sutures.

Source: Martinez et al., 2019.

Finally, we computed an agglomerative clustering tree (Ward's method) to visualize the pairwise angular differences between species' sexual allometric vectors. *Papio papio* was not included in this tree due to its differing sample size of males and females, which is virtually all males (Table 1). Because males and females *Papio* and *Theropithecus* are drastically different in their cranial morphology, we perform separate analyses to explore the general trends when comparing *Papio* males with *Theropithecus* males, and *Papio* females with *Theropithecus* females. These comparisons allow us to independently study the allometric and non-allometric components, and to specifically compare the allometric vectors related to sex for each species by assessing the angular relation between these vectors. All the procedures were performed using MorphoJ version 1.08 (Klingenberg, 2011). Scatterplots were computed in R (R Core Team, 2017, see Supplementary Data). The clustering tree was computed using PAST version 4.15 (Hammer et al., 2001).

Results

PCA before adjusting for size

Figure 2 shows the distribution pattern of all the specimens in the sample, using PCA before adjusting for centroid size. The principal component 1 (PC1) explains the largest amount of variation (43.4%), and it is highly correlated with centroid size (r = 0.91). The PC1 and PC2 together separate the two genera. *Theropithecus* samples cluster in a well-defined area of the PC1/PC2 plot. The *Theropithecus* samples show an important degree of proximity with *Papio*, notably with several *P. hamadryas* males. Some specimens of the genus *Papio* (spp. or unknown species) are confounded with the *Theropithecus* cloud, but this may be due to museum/collection mislabeling. The males of the greater sized species *P. anubis*, *P. ursinus* and most of the *P. cynocephalus* show a higher level of grouping than females. Whereas *P. papio* and *P. hamadryas*, the medium sized species, are intermediate between the larger and smaller ones, like *P. kindae*. The kinda individuals appear near the negative end of PC1 next to some specimens of *P. cynocephalus*. The few *P. cynocephalus* individuals clustering with *P. kindae* are most likely museum/collection mislabeling due to taxonomic nomenclature that predates the raise of kinda from subspecies of *P. cynocephalus* to species *per se* (see Martinez et al., 2019). Likewise, *T. gelada* appears near the same
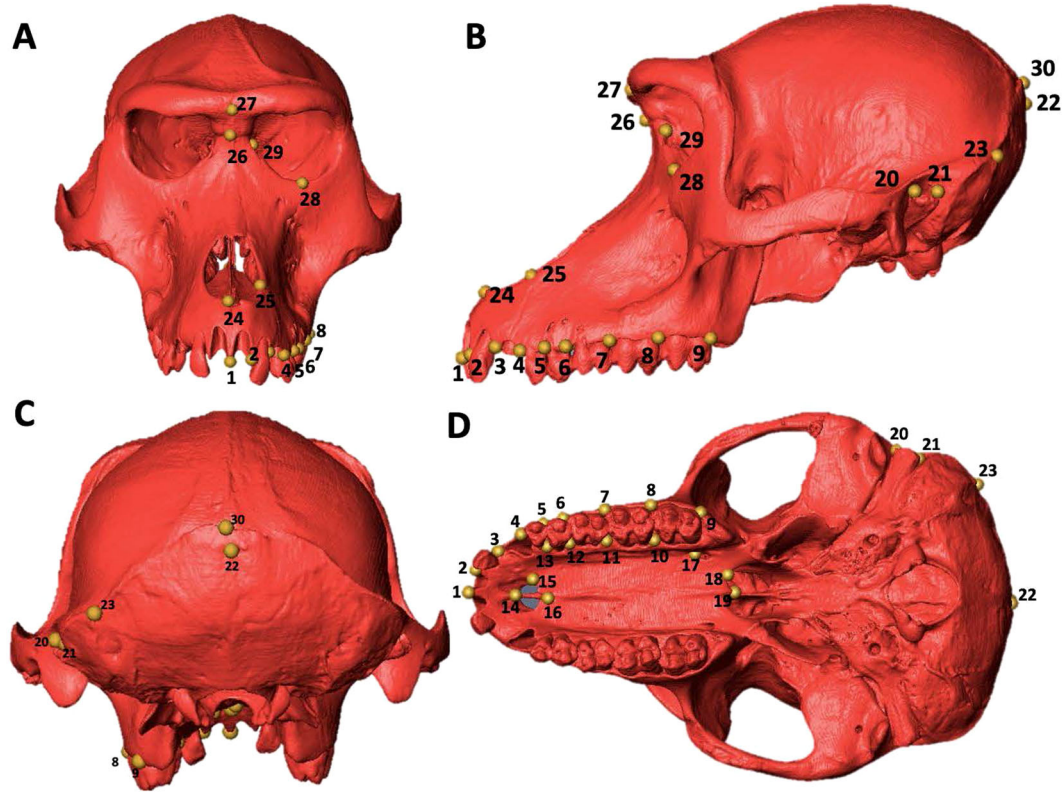

FIGURE 1
Homology map on the skull of a female *Theropithecus gelada* (reference individual: 1091; see the Supplementary Material). **(A)** frontal view. **(B)** lateral view. **(C)** posterior view. **(D)** inferior view.
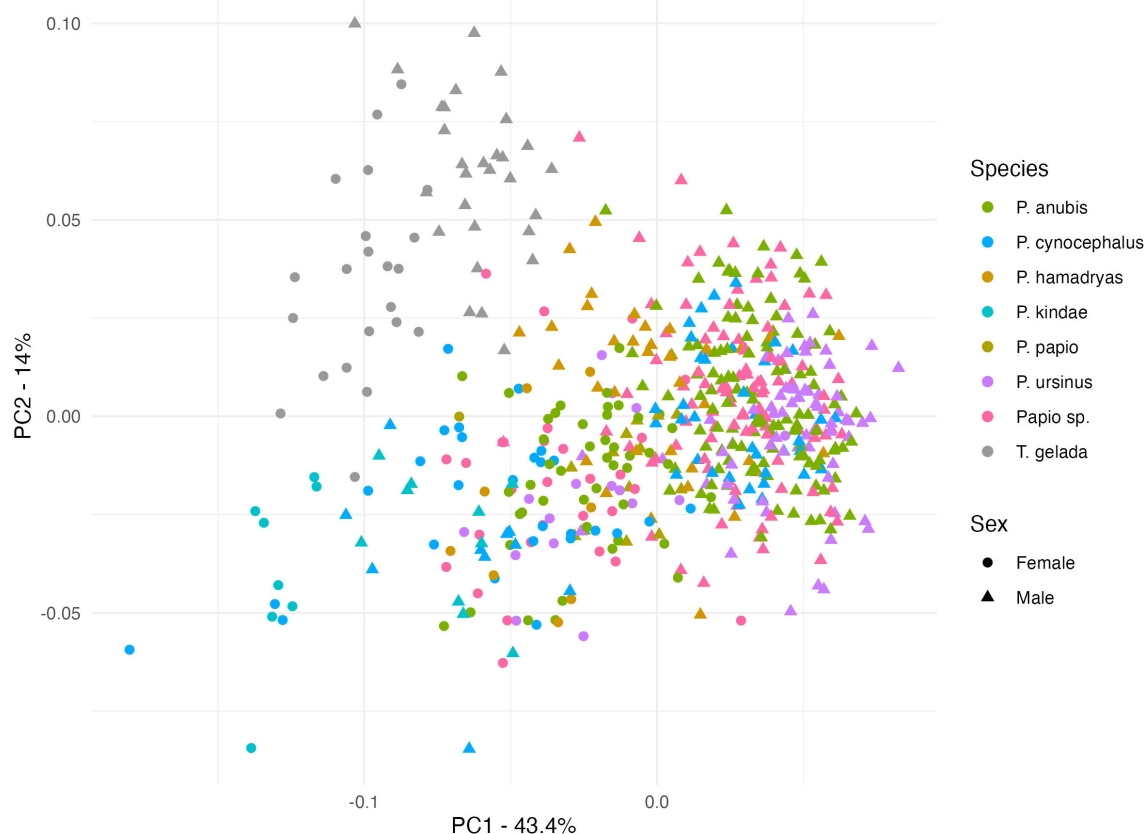
FIGURE 2
Principal component plot with males and females before adjusting for size. Principal Component 1 (PC1) explains the largest amount of variation (43.4%), significantly more than the variance explained by PC2 (14%).

values of PC1 as *P. kindae* but separates from them with higher scores across the PC2.

Sexual dimorphism produces relevant morphological disparity. Therefore, we examine the shape patterns within each sex alone (Figures 3, 4). Figure 3 shows the PC1/PC2 distribution of male individuals. The species with a greater body size like *P. anubis* and *P. ursinus* show higher values in PC1, grouping in the positive end of the distribution. *P. cynocephalus* (also considered big sized Papionini) appears near the same values but with some specimens displaced to the medium and negative scores near *P. hamadryas* and *P. kindae* respectively. As in the previous PCA, the male *Theropithecus* cluster shows an important degree of proximity with *Papio*, notably *P. hamadryas* males. The PC1/PC2 distribution of females (Figure 4) shows a clearer distinction between both genera than males.

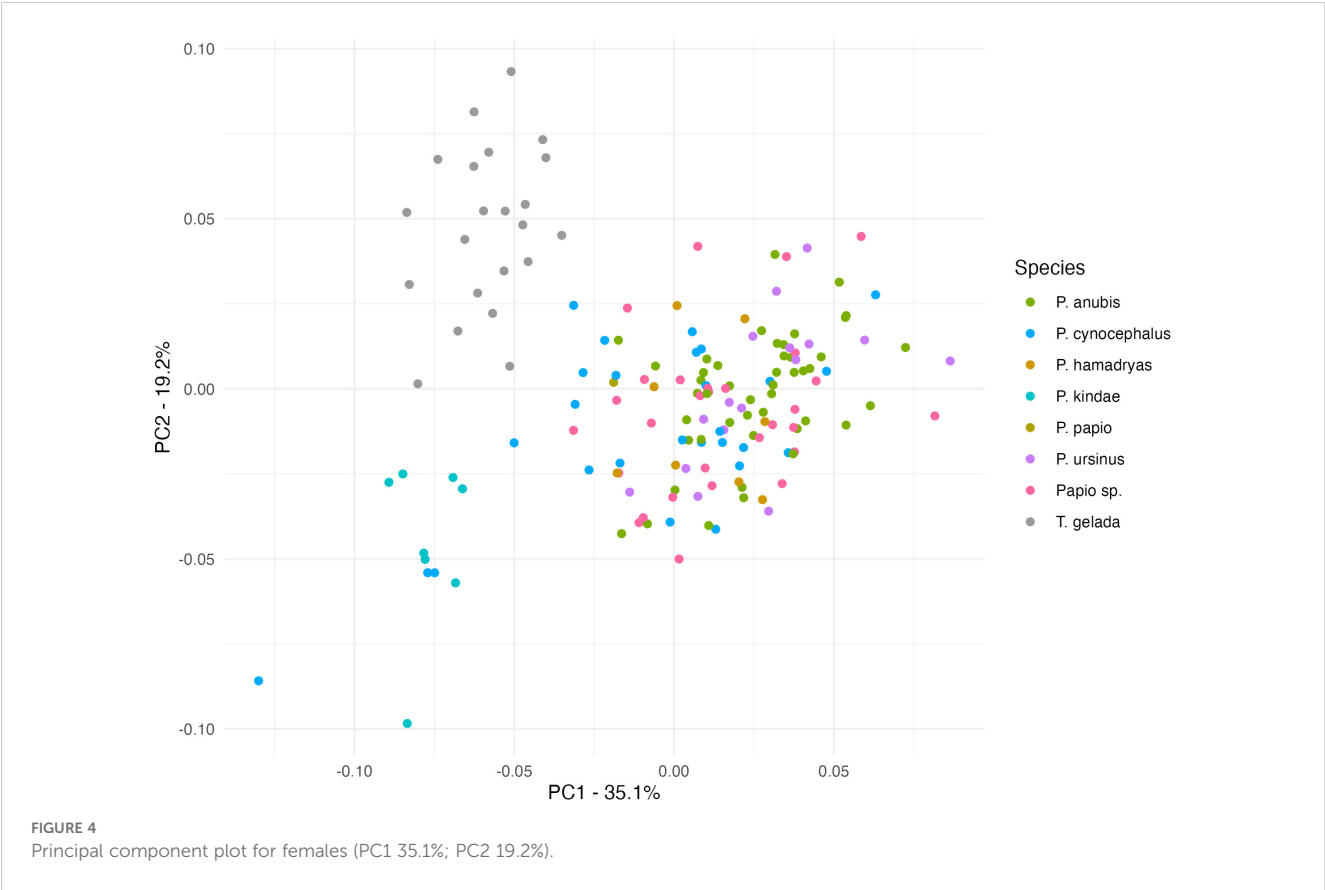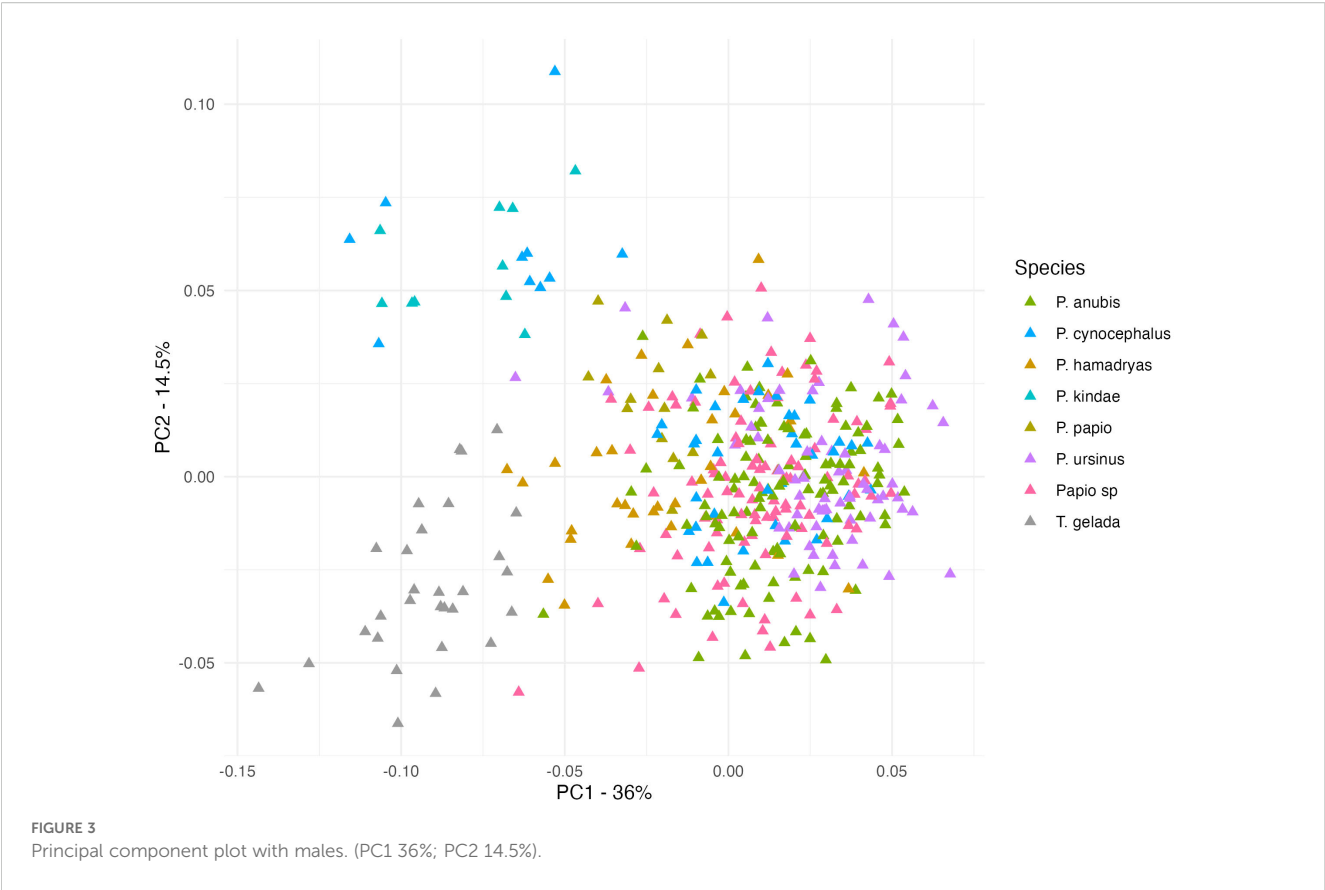## Multivariate regression on size and PCA after adjusting for size

Figures 5 and 6 show the multivariate regression on natural log-centroid size for males and females, respectively. The relationship between shape and size (Regression Score) is summarized from the pooled within-groups multivariate regression of Procrustes

coordinates on the natural log-transformed centroid size. In males, the regression score accounts for 13.2% of the predicted variance and 17.6% in females (p < 0.0001).

Figure 7 shows the distribution pattern of male specimens after adjusting for natural log-centroid size. The principal component 1 (PC1) explains 28.3% and PC2 12.9% of variation. Once the effect of size is adjusted for, the amount of variation explained by PC1 is heavily reduced and the *Theropithecus* clustering now shows a clear separation with *Papio*. A similar situation is observed for females in Figure 8 (PC1/PC2). When the effect of size is removed, the amount of variation explained by PC1 is reduced and the female *Theropithecus* clustering shows a clear distance from the *Papio* clustering.

Centroid size comparison and angular comparison of allometric vectors

We computed a box-plot visualization of centroid size by sex within species in order to observe the pattern of sex-differences in craniofacial size (Figure 9). The most important differences in craniofacial size (centroid size) within species is found (in descending order) in *Papio ursinus*, *Papio anubis*, *Papio cynocephalus*, *Papio papio*, *Papio hamadryas* and *Papio kindae*. It
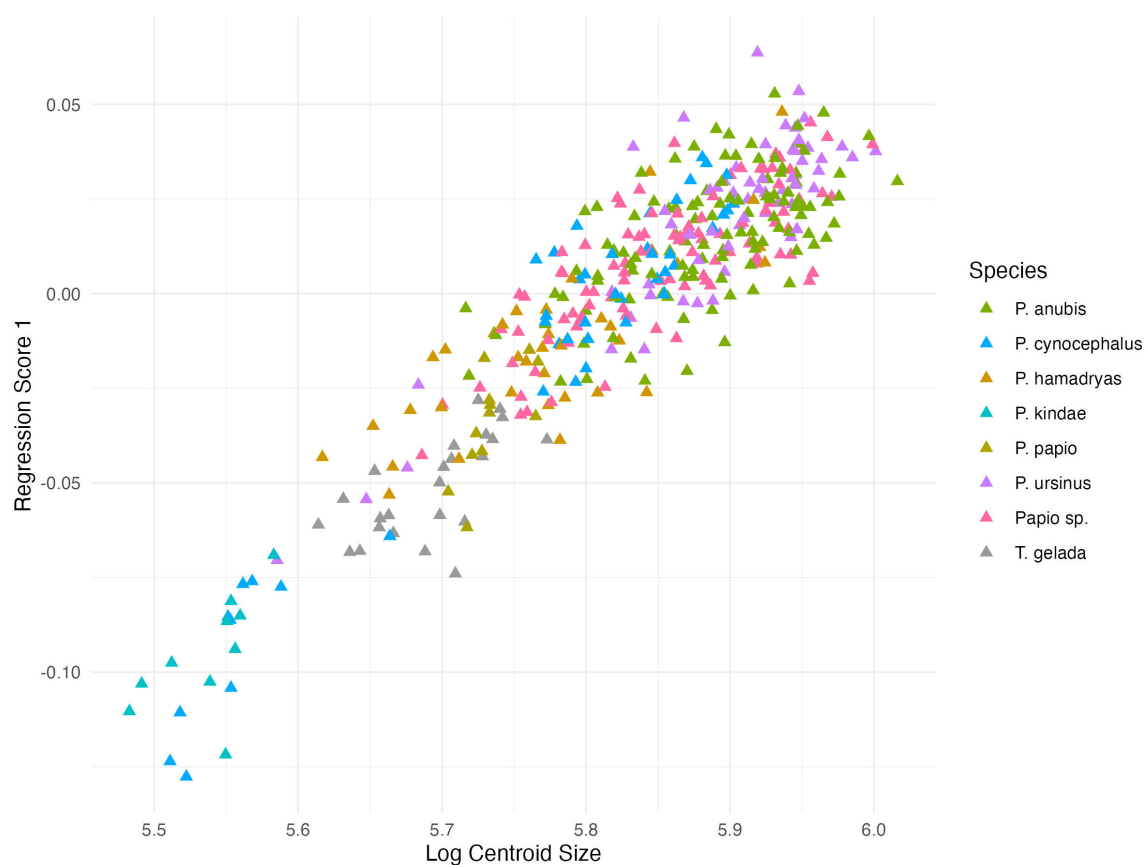
FIGURE 3
Principal component plot with males. (PC1 36%; PC2 14.5%).

FIGURE 4
Principal component plot for females (PC1 35.1%; PC2 19.2%).

FIGURE 5
Regression score (RS) and log centroid size plot for males. RS accounts for 13.2% of the predicted variance (p < 0.0001).

is interesting to note that, despite of being the size of *P. papio* males and *P. cynocephalus* females, *Theropithecus gelada* shows a relational difference in craniofacial size between males and females (i.e. degree of craniofacial sexual dimorphism excluding canines) that is similar to the smaller *Papio kindae*.

In order to compute the allometric vectors for each species, we performed log-centroid size regressions for each separate species, including males and females together in each of these regressions. As stated before, by including males and females together, the resulting shape scores are allometric vectors mostly related to sex differences. In this manner, by assessing the angular relation between shape score vectors, we can obtain pairwise species comparisons of sexual allometric vectors (Singleton et al., 2017; Klingenberg and Marugán-Lobón, 2013). The results are presented in Table 3. All the pairwise comparisons are highly significant (p<0.00001) showing that in all the cases, the observed angle between the two vectors was smaller than expected, suggesting some degree of similarity between them (Klingenberg and Marugán-Lobón, 2013). In order to visualize the magnitude differences of these angular comparisons, we performed an agglomerative clustering tree (Ward's method, Figure 10). We excluded the *P. papio* species in the clustering tree due to its low number of females (only 1 specimen), which distorted the analysis.

Discussion

This study aimed to compare cranial sexual dimorphism between the genera *Papio* and *Theropithecus*. Using geometric morphometric methods: PCA, regression, centroid size and angular comparisons, we described the patterns of size and shape variation in craniofacial dimorphism and assessed their relationship to phylogeny and social structure. Our findings corroborate previous studies that highlighted the importance of allometry in structuring adult craniofacial morphology in papionins (Singleton, 2002; Frost et al., 2003; Dunn et al., 2013). However, by integrating data across all extant *Papio* species and *Theropithecus gelada*, this study reveals critical insights into the evolutionary dynamics of sexual dimorphism that transcend the simple documentation of morphological differences.

The PCA plots before adjusting for size (Figures 2–4) show distinct morphological clusters for each genus, although some degree of overlap is observed. After adjusting for size (Figures 7, 8), a clearer separation emerges, indicating that non-size-related aspects of craniofacial morphology, particularly in midfacial projection and neurocranial proportions, retain genus-specific configurations (Singleton, 2002; Frost et al., 2003). These findings demonstrate that while size strongly influences craniofacial shape,
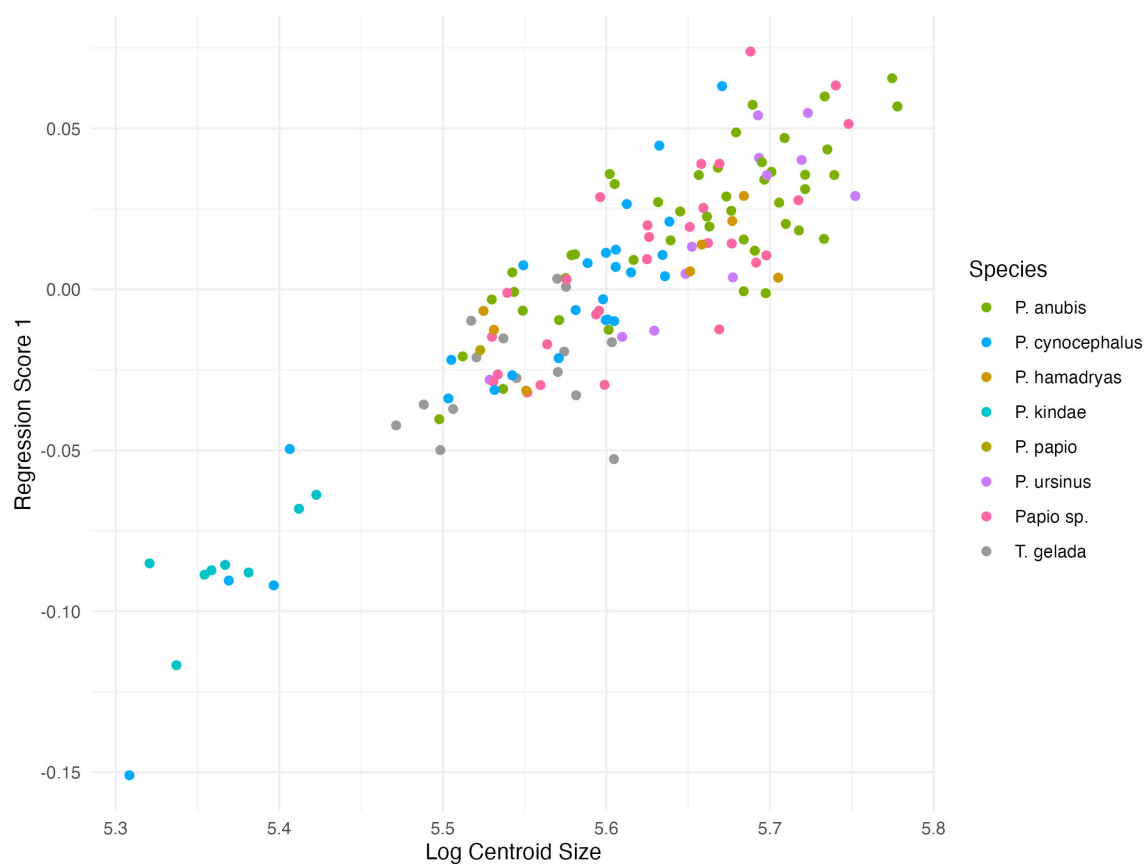
FIGURE 6
Regression score (RS) and log centroid size plot for females. RS accounts for 17.6% of the predicted variance (p < 0.0001).

certain structural features are conserved and diagnostic, reflecting deeper phylogenetic divergence rather than solely functional or ecological convergence. This pattern suggests that the evolutionary history of these lineages has produced distinct morphological signatures that persist despite similar selective pressures, a finding consistent with previous research on papionin cranial morphology (Frost et al., 2003; Singleton, 2002).

The position of *T. gelada* relative to *Papio* species provides particularly novel insights into the evolution of craniofacial dimorphism. Our results indicate that *Theropithecus gelada* represents more than simply another case of sexual dimorphism already documented in *Papio* species. Despite cranial size values comparable to *P. papio* males and *P. cynocephalus* females, *T. gelada* exhibits a degree of sexual dimorphism in craniofacial size that is closer to the smaller *P. kindae* (Figure 9). This unexpected convergence in dimorphism magnitude between *T. gelada* and *P. kindae* represents a distinct pattern worth highlighting, as it challenges the assumption that body size alone predicts the magnitude of craniofacial dimorphism.

This finding is especially significant when considering the contrasting social systems of these species. While *P. kindae* displays reduced sexual dimorphism associated with lower male-male competition and a polygynandrous mating system (Petersdorf et al., 2019), *T. gelada* lives in a multilevel society with intense male

competition for reproductive access (Snyder-Mackler et al., 2012, 2014). The convergence in dimorphism magnitude, despite these contrasting social systems, suggests that multiple evolutionary pathways can produce similar morphological outcomes. This challenges simplistic models that directly link social organization to morphological dimorphism and indicates that the relationship between social structure and morphology is more complex than previously recognized.

The shared aspects of shape dimorphism between *Papio* and *Theropithecus* are primarily related to facial elongation, muzzle robusticity, and neurocranial proportions, consistent with previous studies (Singleton, 2002; Frost et al., 2003). However, our analysis reveals that these similarities manifest differently in each genus, with *T. gelada* showing distinctive patterns in the relative proportions of these features. This suggests that while the basic developmental and functional constraints shaping dimorphism are conserved across papionins, lineage-specific modifications have occurred during the separate evolutionary histories of these genera.

The comparison of allometric vectors and the resulting phenogram (Figure 10) reveal a strong phylogenetic imprint on craniofacial sexual dimorphism. Species cluster in a manner broadly consistent with their molecular relationships (e.g., Rogers et al., 2019; Santander et al., 2022; Mutti et al., 2023), indicating that evolutionary history constrains morphological trajectories even

FIGURE 7
Principal component analysis plot of 'size adjusted shape (using the regression residuals) for males (PC1 28.3%; PC2 12.9%).

across lineages with diverse ecological and social adaptations. This finding supports the hypothesis that phylogenetic history is a primary driver of sexual dimorphism patterns in papionins, providing a framework within which functional adaptations can evolve (Frost et al., 2003; Gilbert et al., 2009).

This observation is important for understanding baboon evolution and ecology because it demonstrates how ecological specialization can drive morphological divergence even within a framework of phylogenetic constraint (Fleagle, 2013). Our findings address a fundamental evolutionary question: is phylogenetic history the primary driver of sexual dimorphism patterns, or are functional factors, such as social organization and ecological specialization, equally or more influential? Previous studies in diverse primate groups have demonstrated that ecological specialization acts as an important driver of morphological divergence and speciation (Kamilar and Cooper, 2013; Cardini and Elton, 2008). Specific dietary adaptations have been shown to have profound effects on primate craniofacial morphology, as documented by Ross et al. (2012) and Ravosa et al. (2016), who found that dietary specializations produce significant changes in mandibular biomechanics and facial structure, even in closely related lineages. For example, Kamilar and Cooper (2013) documented how dietary adaptations in primates lead to specific

craniofacial modifications that can evolve rapidly in response to ecological pressures, even when phylogenetic constraints exist. The evidence suggests a complex interplay between these factors, where the broad conservation of dimorphism patterns across papionins points to phylogenetic constraint, while the specific manifestations of dimorphism in each lineage reflect adaptations to particular ecological and social contexts.

Taken together, our findings demonstrate that craniofacial sexual dimorphism in these genera is broadly conserved in magnitude but varies in morphological expression between lineages. This highlights the importance of considering both phylogenetic history and functional/ecological context when interpreting patterns of sexual dimorphism. The case of *Theropithecus gelada* is particularly instructive, as it represents a distinct evolutionary experiment in which similar degrees of dimorphism to certain *Papio* species have evolved in the context of different ecological specializations and social structures.

Understanding how craniofacial features evolve under competing pressures from sexual selection, ecological adaptation, and phylogenetic inertia will require future research that integrates genomic, developmental, and behavioral data. Our study provides a foundation for these future investigations by demonstrating that the evolution of sexual dimorphism in closely related primates follows
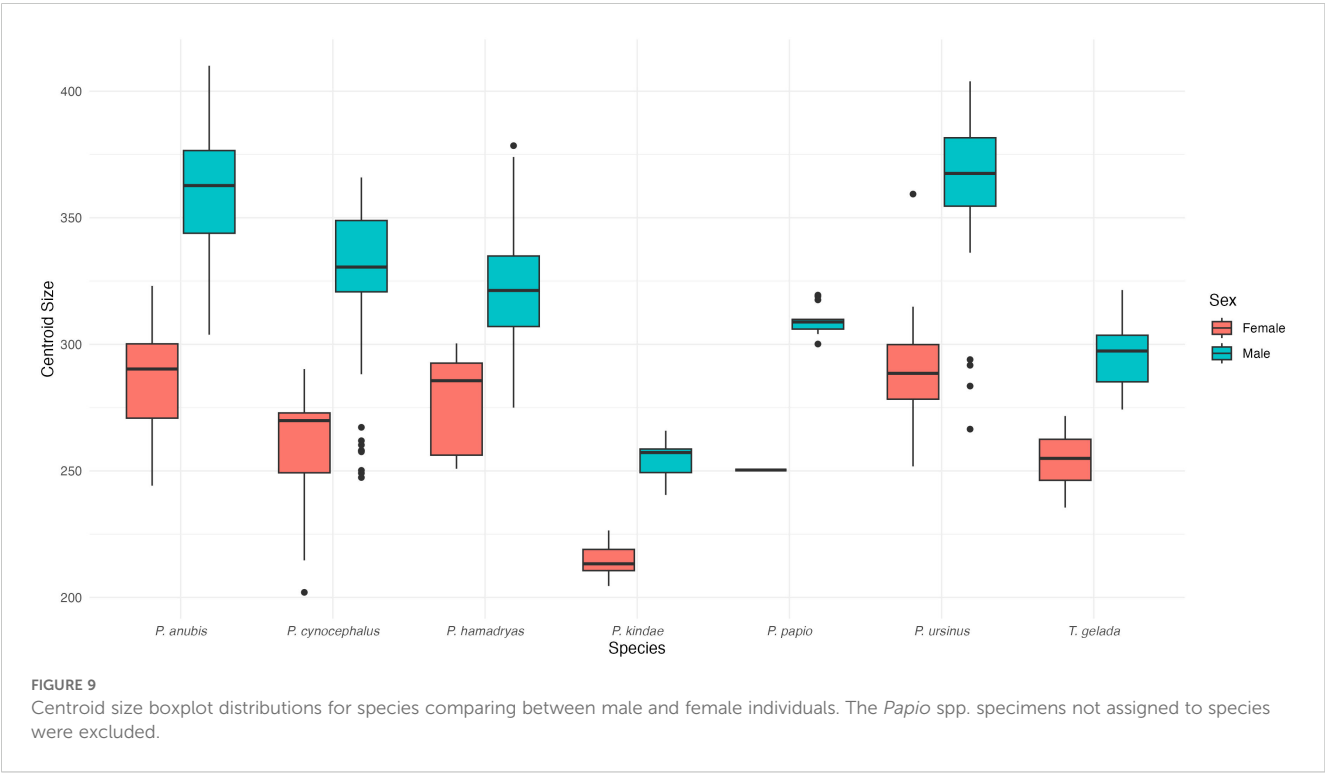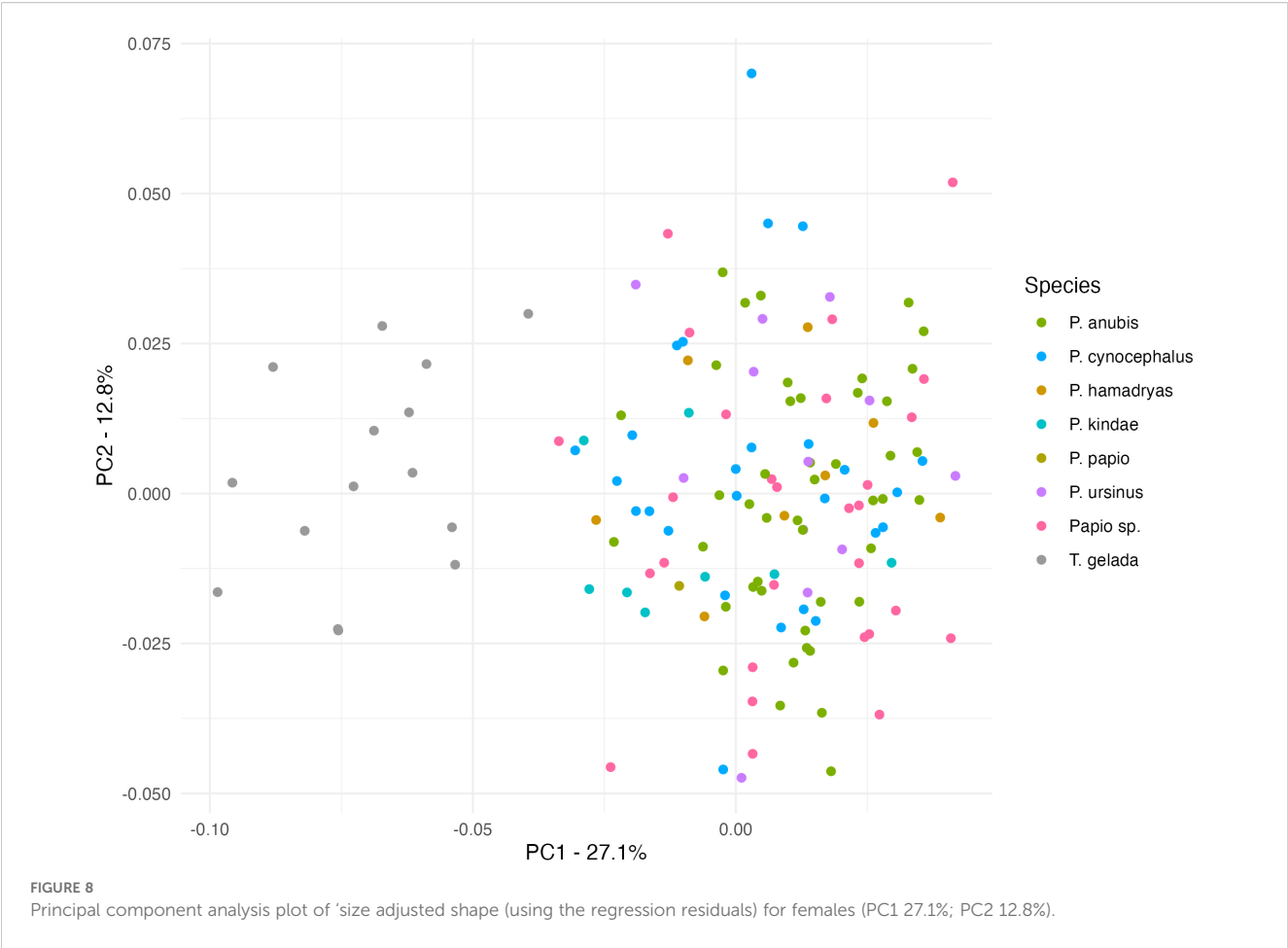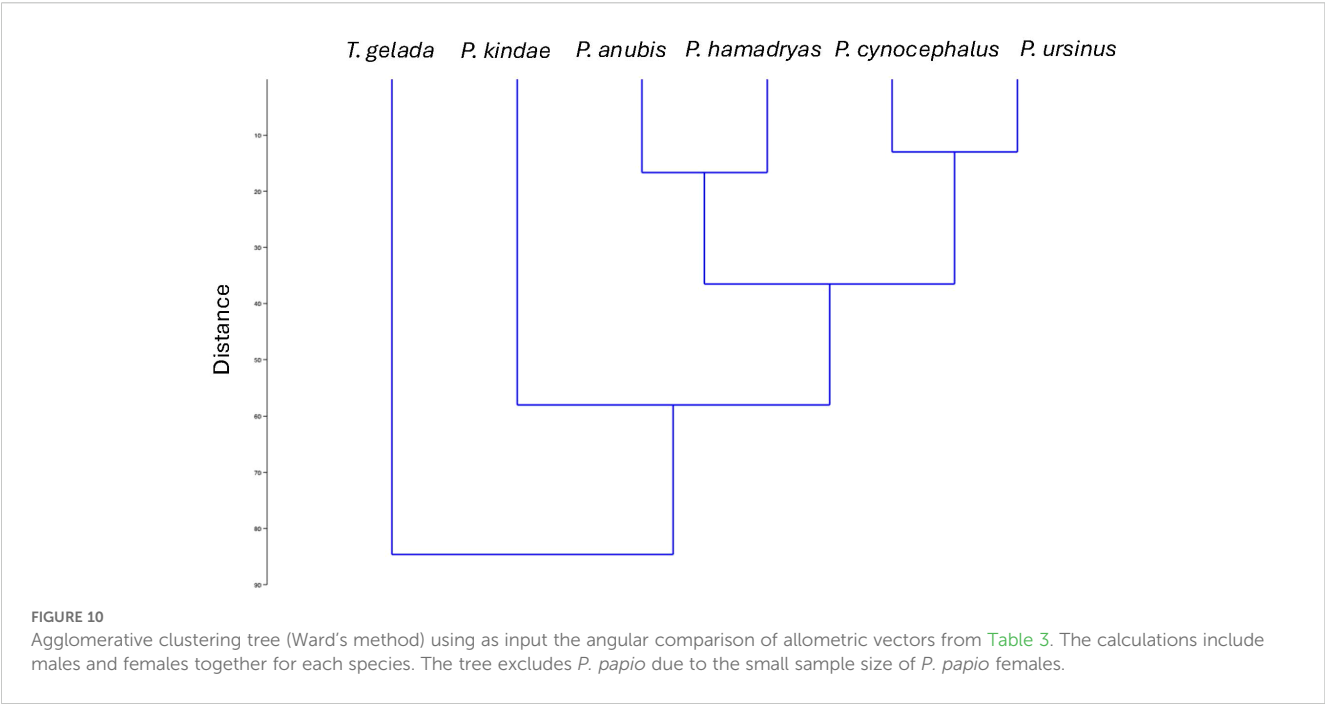
FIGURE 8
Principal component analysis plot of 'size adjusted shape (using the regression residuals) for females (PC1 27.1%; PC2 12.8%).

FIGURE 9
Centroid size boxplot distributions for species comparing between male and female individuals. The *Papio* spp. specimens not assigned to species were excluded.

TABLE 3 Angular comparison of allometric vectors.

Species	T. gelada	P. anubis	P. hamadryas	P. papio	P. cynocephalus	P. ursinus	P. kindae
T. gelada	0	35.306	42.358	58.932	43.881	42.424	49.66
P. anubis	35.306	0	15.529	41.593	20.844	19.199	35.091
P. hamadryas	42.358	15.529	0	42.349	21.809	23.924	36.12
P. papio	58.932	41.593	42.349	0	41.037	40.099	34.417
P. cynocephalus	43.881	20.844	21.809	41.037	0	12.682	28.431
P. ursinus	42.424	19.199	23.924	40.099	12.682	0	31.136
P. kindae	49.66	35.091	36.12	34.417	28.431	31.136	0
All Papio sp.	41.906						

All p values <0.00001.

FIGURE 10
Agglomerative clustering tree (Ward's method) using as input the angular comparison of allometric vectors from Table 3. The calculations include males and females together for each species. The tree excludes *P. papio* due to the small sample size of *P. papio* females.

complex pathways that cannot be reduced to simple correlations with body size or social system. This complexity reflects the multifaceted nature of selection pressures acting on primate morphology and underscores the value of comparative studies in elucidating evolutionary processes.

Data availability statement

The raw data supporting the conclusions of this article will be made available by the authors, without undue reservation.

Ethics statement

The animal study was approved by Comité Ético Científico para el Cuidado de Animales y Ambiente, Pontificia Universidad Católica de Chile. The study was conducted in accordance with the local legislation and institutional requirements.

Author contributions

ÁO: Conceptualization, Data curation, Formal analysis, Investigation, Methodology, Writing – original draft, Writing – review & editing, Visualization, Software. AF-T: Conceptualization, Data curation, Formal analysis, Investigation, Methodology, Software, Visualization, Writing – original draft, Writing – review & editing. RoB: Conceptualization, Data curation, Formal analysis, Investigation, Methodology, Visualization, Writing – original draft, Writing – review & editing, Software. MC: Data curation, Methodology, Writing – review & editing. JM: Writing – review & editing, Investigation, Methodology. GD: Data curation, Methodology, Writing – review & editing, Resources. SG: Data

Funding

Acknowledgments

Conflict of interest

The authors declare that the research was conducted in the absence of any commercial or financial relationships that could be construed as a potential conflict of interest.

Generative AI statement

The author(s) declare that no Generative AI was used in the creation of this manuscript.

Any alternative text (alt text) provided alongside figures in this article has been generated by Frontiers with the support of artificial intelligence and reasonable efforts have been made to ensure accuracy, including review by the authors wherever possible. If you identify any issues, please contact us.

Publisher's note

All claims expressed in this article are solely those of the authors and do not necessarily represent those of their affiliated organizations, or those of the publisher, the editors and the reviewers. Any product that may be evaluated in this article, or claim that may be made by its manufacturer, is not guaranteed or endorsed by the publisher.

Supplementary material

The Supplementary Material for this article can be found online at: https://www.frontiersin.org/articles/10.3389/fevo.2025.1537474/full#supplementary-material

References

Alberts, S. C., Buchan, J. C., and Altmann, J. (2006). Sexual selection in wild baboons: from mating opportunities to paternity success. *Anim. Behav.* 72, 1177–1196. doi: 10.1016/j.anbehav.2006.05.001

Alberts, S. C., Watts, H. E., and Altmann, J. (2003). Queuing and queue-jumping: long-term patterns of reproductive skew in male savannah baboons, *Papio cynocephalus*. *Anim. Behav.* 65, 821–840. doi: 10.1006/anbe.2003.2106

Bergman, T. J., and Beehner, J. C. (2013). *Theropithecus gelada* (Gelada baboon). In: *Mammals of Africa. Primates* 2, 240–244.

Bobe, R., Martínez, F. I., and Carvalho, S. (2020). Primate adaptations and evolution in the southern African Rift Valley. *Evol. Anthropol.* 29, 94–101. doi: 10.1002/evan.21826

Bookstein, F. L. (1991). *Morphometric Tools for Landmark Data: Geometry and Biology*. Cambridge: Cambridge University Press.

Bulger, J. B. (1993). Dominance rank and access to estrous females in male savanna baboons. *Behaviour* 127, 67–103. doi: 10.1163/156853993X00434

Caldon, M., Mercuri, G., Mutti, G., da Silva, M. J. F., Martinez, F. I., and Capelli, C. (2025). Baboons at a crossroads: hybridisation events and genomic links of central Mozambique's baboons with papio neighbors. *Am. J. Biol. Anthropol.* 187, e70082. doi: 10.1002/ajpa.70082

Caldon, M., Mutti, G., Mondanaro, A., Imai, H., Shotake, T., Oteo Garcia, G., et al (2024). Gelada genomes highlight events of gene flow, hybridisation and local adaptation that track past climatic changes. *Mol. Ecol.* 33 (19), e17514. doi: 10.1111/mec.17514

Cardini, A., and Elton, S. (2008). Does the skull carry a phylogenetic signal? Evolution and modularity in the guenons. *Biol. J. Linn. Soc.* 93, 813–834. doi: 10.1111/j.1095-8312.2008.01011.x

Chowdhury, S., Pines, M., Saunders, J., and Swedell, L. (2015). The adaptive value of secondary males in the polygynous multi-level society of hamadryas baboons. *Am. J. Phys. Anthropol.* 158, 501–513. doi: 10.1002/ajpa.22804

Collard, M., and O'Higgins, P. (2001). Ontogeny and homoplasy in the papionin monkey face. *Evol. Dev.* 3, 322–331. doi: 10.1046/j.1525-142x.2001.01042.x

Copes, L. E., Lucas, L. M., Thostenson, J. O., Hoekstra, H. E., and Boyer, D. M. (2016). A collection of non-human primate computed tomography scans housed in MorphoSource, a repository for 3D data. *Sci. Data* 3, 160001. doi: 10.1038/sdata.2016.1

Craig, J. M., Hedges, S. B., and Kumar, S. (2024). Completing a molecular timetree of primates. *Front. Bioinform.* 4. doi: 10.3389/fbinf.2024.1495417

Delson, E., Terranova, C. J., Jungers, W. L., Sargis, E. J., Jablonski, N. G., and Dechow, P. C. (2000). Body mass in Cercopithecidae (Primates, Mammalia): estimation and scaling in extinct and extant taxa. *Anthropol. Pap. Am. Mus.* 83, 1–159.

Dixson, A. F. (2012). *Primate Sexuality: Comparative Studies of the Prosimians, Monkeys, Apes, and Humans. 2nd edition* (Oxford: Oxford University Press).

Dixson, A. F. (2017). Copulatory and postcopulatory sexual selection in primates. *Folia Primatol.* 89, 258–286. doi: 10.1159/000488105

Drake, A. G., and Klingenberg, C. P. (2008). The pace of morphological change: historical transformation of skull shape in St Bernard dogs. *Proc. R. Soc. B* 275, 71e76. doi: 10.1098/rspb.2007.1169

Dunbar, R. I. M. (1990). Environmental determinants of intraspecific variation in body weight in baboons (*Papio* spp.). *J. Zool.* 220, 157–169. doi: 10.1111/j.1469-7998.1990.tb04300.x

Dunbar, R. I. M., and Dunbar, E. P. (1974). On hybridization between *Theropithecus gelada* and *Papio anubis* in the wild. *J. Hum. Evol.* 3, 187–192. doi: 10.1016/0047-2484(74)90176-6

Dunn, J., Cardini, A., and Elton, S. (2013). Biogeographic variation in the baboon: dissecting the cline. *J. Anat.* 223, 337–352. doi: 10.1111/joa.12085

Elton, S., and Cardini, A. (2008). Anthropology from the desk? The challenges of the emerging era of data sharing. *J. Anthropol. Sci.* 86, 209–212.

Elton, S., and Dunn, J. (2020). Baboon biogeography, divergence, and evolution: Morphological and paleoecological perspectives. *J. Hum. Evol.* 145, 102799. doi: 10.1016/j.jhevol.2020.102799

Ferreira da Silva, M. J., Tralma, P., Colmonero-Costeira, I., Cravo-Mota, M., Farassi, R., Hammond, P., et al. (2025). Sex-mediated Gene Flow in Grayfoot Chacma Baboons (*Papio ursinus griseipes*) in Gorongosa National Park, Mozambique. *Int. J. Primatol.* 46, 705–736. doi: 10.1007/s10764-025-00494-2

Fischer, J., Higham, J. P., Alberts, S. C., Barrett, L., Beehner, J. C., Bergman, T. J., et al. (2019). Insights into the evolution of social systems and species from baboon studies. *eLife* 8, e50989. doi: 10.7554/eLife.50989

Fischer, J., Kopp, G. H., Dal Pesco, F., Goffe, A., Hammerschmidt, K., Kalbitzer, U., et al. (2017). Charting the neglected West: The social system of Guinea baboons. *Am. J. Phys. Anthropol.* 162, 15–31. doi: 10.1002/ajpa.23144

Fleagle, J. G. (2013). *Primate Adaptation and Evolution* (New York: Academic Press).

Frost, S. R. (2013). Cranial shape variation in extant and fossil *Papio* and its implications for the evolution of the Kinda baboon. *Am. J. Phys. Anthropol.* S56, 126.

Frost, S. R., Marcus, L. F., Bookstein, F. L., Reddy, D. P., and Delson, E. (2003). Cranial allometry, phylogeography, and systematics of large-bodied papionins (Primates: cercopithecinae) inferred from geometric morphometric analysis of landmark data. *Anat. Rec. A Discov. Mol. Cell. Evol. Biol.* 275A, 1048–1072. doi: 10.1002/ar.a.10112

Gilbert, C. C., Frost, S. R., and Strait, D. S. (2009). Allometry, sexual dimorphism, and phylogeny: A cladistic analysis of extant African papionins using craniodental data. *J. Hum. Evol.* 57, 298–320. doi: 10.1016/j.jhevol.2009.05.013

Gilbert, C. C., and Rossie, J. B. (2007). Congruence of molecules and morphology using a narrow allometric approach. *Proc. Natl. Acad. Sci. U.S.A.* 104, 11910–11914. doi: 10.1073/pnas.0702174104

Gippoliti, S. (2010). *Theropithecus gelada* distribution and variations related to taxonomy: history, challenges and implications for conservation. *Primates* 51, 291–297. doi: 10.1007/s10329-010-0202-x

Hammer, Ø., Harper, D. A. T., and Ryan, P. D. (2001). PAST: paleontological statistics software package for education and data analysis. *Paleontologia Electronica* 4, 9. Available online at: https://palaeo-electronica.org/2001_1/past/issue1_01.htm.

Harris, E. E., and Disotell, T. R. (1998). Nuclear gene trees and the phylogenetic relationships of the mangabeys (Primates: Papionini). *Mol. Biol. Evol.* 15, 892–900. doi: 10.1093/oxfordjournals.molbev.a025993

Jolly, C. J. (2020). Philopatry at the frontier: A demographically driven scenario for the evolution of multilevel societies in baboons (*Papio*). *J. Hum. Evol.* 146, 102819. doi: 10.1016/j.jhevol.2020.102819

Jolly, C. J., Burrell, A. S., Bergey, C., and Rogers, J. (2011). Kinda baboons (*Papio kindae*) and grayfoot chacma baboons (*P. ursinus griseipes*) hybridize in the Kafue River Valley, Zambia. *Am. J. Primatol.* 73, 291–303. doi: 10.1002/ajp.20896

Kamilar, J. M., and Cooper, N. (2013). Phylogenetic signal in primate behaviour, ecology and life history. *Philos. Trans. R. Soc. B: Biol. Sci.* 368, 20120341. doi: 10.1098/rstb.2012.0341

Klingenberg, C. P. (2011). MorphoJ: an integrated software package for geometric morphometrics. *Mol. Ecol. Resour.* 11, 353e357. doi: 10.1111/j.1755-0998.2010.02924.x

Klingenberg, C. P., and Marugán-Lobón, J. (2013). Evolutionary covariation in geometric morphometric data: analyzing integration, modularity, and allometry in a phylogenetic context. *Sys. Biol.* 62, 591e610. doi: 10.1093/sysbio/syt025

Kummer, H. (1968). *Social Organization of Hamadryas Baboons* (Chicago: University of Chicago Press).

Leigh, S. R. (2006). Cranial ontogeny of *papio* baboons (*Papio hamadryas*). *Am. J. Phys. Anthropol.* 130, 71–84. doi: 10.1002/ajpa.20319

Leigh, S. R., and Bernstein, R. M. (2006). "Ontogeny, Life History, and Maternal Investment in baboons," in *Reproduction and Fitness in Baboons: Behavioral, Ecological, and Life History Perspectives*. Eds. L. Swedell and S. R. Leigh (Kluwer Academic/Plenum Press, New York), 225–255.

Leigh, S. R., and Cheverud, J. M. (1991). Sexual dimorphism in the baboon facial skeleton. *Am. J. Phys. Anthropol.* 84, 193–208. doi: 10.1002/ajpa.1330840209

Leigh, S. R., Setchell, J. M., and Buchanan, L. S. (2005). Ontogenetic bases of canine dimorphism in anthropoid primates. *Am. J. Phys. Anthropol.* 127, 296–311. doi: 10.1002/ajpa.20096

Liedigk, R., Roos, C., Brameier, M., and Zinner, D. (2014). Mitogenomics of the Old World monkey tribe Papionini. *BMC Evol. Biol.* 14, 176. doi: 10.1186/s12862-014-0176-1

Martinez, F., Capelli, C., Ferreira da Silva, M. J., Aldeias, V., Alemseged, Z., Archer, W., et al. (2019). A missing piece of the *Papio* puzzle: Gorongosa baboon phenostructure and intrageneric relationships. *J. Hum. Evol.* 130, 1–20. doi: 10.1016/j.jhevol.2019.01.007

Mutti, G., Oteo-Garcia, G., Caldon, M., da Silva, M. J. F., Minhós, T., Cowlishaw, G., et al. (2023). Assessing the recovery of Y chromosome microsatellites with population genomic data using *Papio* and *Theropithecus* genomes. *Sci. Rep.* 13, 13839. doi: 10.1038/s41598-023-40931-x

Petersdorf, M., Weyher, A. H., Kamilar, J. M., Dubuc, C., and Higham, J. P. (2019). Sexual selection in the Kinda baboon. *J. Hum. Evol.* 135, 102635. doi: 10.1016/j.jhevol.2019.06.006

Pines, M., Saunders, J., and Swedell, L. (2011). Alternative routes to the leader male role in a multi-level society: follower vs. solitary male strategies and outcomes in hamadryas baboons. *Am. J. Primatol.* 73, 679–691. doi: 10.1002/ajp.20951

Plavcan, J. M. (1998). Correlated response, competition, and female canine size in primates. *Am. J. Phys. Anthropol.* 107 (4), 401–416. doi: 10.1002/(SICI)1096-8644(199812)107:4<401::AID-AJPA3>3.0.CO;2-N

Pugh, K. D., and Gilbert, C. C. (2018). Phylogenetic relationships of living and fossil African papionins: Combined evidence from morphology and molecules. *J. Human. Evol.* 123, 35–51. doi: 10.1016/j.jhevol.2018.06.002

Ravosa, M. J., Menegaz, R. A., Scott, J. E., Daegling, D. J., and McAbee, K. R. (2016). Limitations of a morphological criterion of adaptive inference in the fossil record. *Biol. Rev.* 91, 883–898. doi: 10.1111/brv.12199

R Core Team (2017). *R: A Language and Environment for Statistical Computing* (Vienna: R Foundation for Statistical Computing).

Rogers, J., Raveendran, M., Harris, R. A., Mailund, T., Leppala, K., Athanasiadis, G., et al. (2019). The comparative genomics and complex population history of *Papio* baboons. *Sci. Adv.* 5, eaau6947. doi: 10.1126/sciadv.aau6947

Ross, C. F., Iriarte-Diaz, J., and Nunn, C. L. (2012). Innovative approaches to the relationship between diet and mandibular morphology in primates. *Int. J. Primatol.* 33, 632–660. doi: 10.1007/s10764-012-9599-y

Santander, C., Molinaro, L., Mutti, G., Martínez, F. I., Mathe, J., Ferreira da Silva, M. J., et al. (2022). Genomic variation in baboons from central Mozambique unveils complex evolutionary relationships with other *Papio* species. *BMC Ecol. Evol.* 22, 44. doi: 10.1186/s12862-022-01999-7

Schreier, A. L., and Swedell, L. (2009). The fourth level of social structure in a multi-level society: ecological and social functions of clans in hamadryas baboons. *Am. J. Primatol.* 71, 948–955. doi: 10.1002/ajp.20736

Setchell, J. M. (2005). Do female mandrills prefer brightly colored males? *Int. J. Primatol.* 26, 715–735. doi: 10.1007/s10764-005-5305-7

Setchell, J. M., and Dixson, A. F. (2001). Changes in the secondary sexual adornments of male mandrills (*Mandrillus sphinx*) are associated with gain and loss of alpha status. *Horm. Behav.* 39, 177–184. doi: 10.1006/hbeh.2000.1628

Shotake, T., Saijuntha, W., Agatsuma, T., and Kawamoto, Y. (2016). Genetic diversity within and among gelada (*Theropithecus gelada*) populations based on mitochondrial DNA analysis. *Anthropol. Sci.* 124 (3), 157–167.

Simons, E. A., Frost, S. R., and Singleton, M. (2018). Ontogeny and phylogeny of the cercopithecine cranium: A geometric morphometric approach to comparing shape change trajectories. *J. Hum. Evol.* 124, 40–51. doi: 10.1016/j.jhevol.2018.08.001

Singleton, M. (2002). Patterns of cranial shape variation in the Papionini (Primates: Cercopithecinae). *J. Hum. Evol.* 42, 547–578. doi: 10.1006/jhev.2001.0539

Singleton, M., Seitelman, B. C., Krecioch, J. R., and Frost, S. R. (2017). Cranial sexual dimorphism in the Kinda baboon (*Papio hamadryas kindae*). *Am. J. Phys. Anthropol.* 164, 102635. doi: 10.1002/ajpa.23304

Slice, D. E. (2001). Landmark coordinates aligned by Procrustes analysis do not lie in Kendall's shape space. *Syst. Biol.* 50, 141–149.

Smith, R. J., and Jungers, W. L. (1997). Body mass in comparative primatology. *J. Hum. Evol.* 32, 523–559. doi: 10.1006/jhevol.1996.0122

Snyder-Mackler, N., Alberts, S. C., and Bergman, T. J. (2014). The socio-genetics of a complex society: female gelada relatedness patterns mirror association patterns in a multilevel society. *Mol. Ecol.* 23, 6179–6191. doi: 10.1111/mec.12987

Snyder-Mackler, N., Beehner, J. C., and Bergman, T. J. (2012). Defining higher levels in the multilevel societies of geladas (*Theropithecus gelada*). *Int. J. Primatol.* 33, 1054–1068. doi: 10.1007/s10764-012-9584-5

Strasser, E., and Delson, E. (1987). Cladistic analysis of cercopithecid relationships. *J. Hum. Evol.* 16, 81–99. doi: 10.1016/0047-2484(87)90061-3

Swedell, L. (2011). "African Papionins: Diversity of Social Organization and Ecological Flexibility," in *Primates in Perspective*, vol. 2. Eds. C. J. Campbell, A. Fuentes, K. C. MacKinnon, S. K. Bearder and R. M. Stumpf (Oxford University Press, Oxford), 241–277.

Trede, F., Lemkul, A., Atickem, A., Beehner, J. C., Bergman, T. J., Burke, R. J., et al. (2020). Geographic distribution of microsatellite alleles in geladas (primates, Cercopithecidae): Evidence for three evolutionary units. *Zoologica Scripta* 49, 659–667. doi: 10.1111/zsc.12451

Walker, J. A., Jordan, V. E., Storer, J. M., Steely, C. J., Gonzalez-Quiroga, P., Beckstrom, T. O., et al. (2019). Alu insertion polymorphisms shared by *Papio* baboons and *Theropithecus gelada* reveal an intertwined common ancestry. *Mob. DNA.* 10, 46. doi: 10.1186/s13100-019-0187-y

Zinner, D., Arnold, M. L., and Roos, C. (2011). The strange blood: natural hybridization in primates. *Evol. Anthropol.* 20, 96–103. doi: 10.1002/evan.20301

Zinner, D., Atickem, A., Beehner, J. C., Bekele, A., Bergman, T. J., Burke, R., et al. (2018). Phylogeography, mitochondrial DNA diversity, and demographic history of geladas (*Theropithecus gelada*). *PloS One* 13, e0202303. doi: 10.1371/journal.pone.0202303

Zinner, D., Fickenscher, G., and Roos, C. (2013). "Family Cercopithecidae (Old World Monkeys)," in *The Handbook of the Mammals of the World, Primates*, vol. 3. Eds. R. A. Mittermeier, A. B. Rylands and D. E. Wilson (Lynx Edicions, Barcelona), 550–627.

Zinner, D., Groeneveld, L. F., Keller, C., and Roos, C. (2009). Mitochondrial phylogeography of baboons (*Papio* spp.): indication for introgressive hybridization? *BMC Evol. Biol.* 9, 83. doi: 10.1186/1471-2148-9-83